European Conference on Optical Communication (ECOC) 2022 © Optica Publishing Group 2022

Less Than 0.03 dB Multicore Fiber Passive Fusion Splicing Using New Azimuthal Alignment Algorithm and 3-Electrode Arc-Discharging System

Tristan Kremp[(1)], Yue Liang[(2)], Alan H. McCurdy[(2)]

[(1)] OFS Laboratories, Somerset, NJ, USA, tkremp@ofsoptics.com
[(2)] OFS Fitel, LLC, Norcross, GA, USA

Abstract *We present a novel azimuthal alignment algorithm for multicore fiber splicing that separates the core and marker information in side-view images. For two different 4-core fiber designs, average fusion splice losses of less than 0.03 dB are demonstrated using a 3-electrode arc-discharging fusion splicer. ©2022 The Author(s)*

Introduction

Multicore fiber (MCF) continues to gain interest due to the need for higher spatial density as bandwidth demands grow exponentially while the available space, e.g., in the ducts of hyperscale data centers or inside the armored protection layer of submarine communication cables, is limited. Fast, low-loss and high-strength splicing capabilities are key requirements for the deployment, but existing splicing algorithms and machines tend to have problems in consistently and precisely aligning the correct cores of the two MCF to be spliced. Using the cross-correlation of side-view images for 4-core or 8-core fibers, fusion splice losses of about 0.5 dB were reported in [1], which these authors found to be comparable to the results from splicing with active feedback that monitors the insertion loss during the alignment optimization. Lower splice losses of 0.08–0.18 dB for the center core and 0.1–1.0 dB for the six outer cores of a symmetric 7-core fiber were reported in [2] using a so-called interrelation profile analysis (IPA) method [3]. With an improved IPA2 version of this method, an average splice loss of 0.092 dB for a 4-core fiber with marker [4] and 0.2 dB with 80% success rate for a low-crosstalk trench-assisted 4-core fiber with marker [5] were achieved. With a field-usable compact fusion splicer, 0.12dB splice loss were achieved [6] for a 5-core fiber. Reverse-tapering the smaller of two spacing-mismatched 7-core fibers, 0.17dB insertion loss were reported in [7]. Applying a similar thermal technique that expands the cross section at the ends of two identical coupled-core 4-core fibers, a minimum splice loss of 0.02dB has been achieved [8], but at the expense of increasing the power coupling between cores by 20 dB, which may be beneficial for such coupled-core MCF, but is detrimental for uncoupled-core MCF applications where channel crosstalk should be minimized. A Fourier-based method for fibers with 180-degree periodicity, e.g., polarization maintaining fibers with stress rods, has been suggested in [9], achieving an azimuthal angle error of (1.06±0.92) degrees. While all these methods were side-view based, an end-view based method [10] was reported to give an average fusion splice loss of 0.09dB for the inner core and 0.18 dB for the outer cores of a dual-ring 12-core fiber.

However, these values are substantially higher than typical single-core fiber splice losses, which are usually below 0.03 dB for core alignment and around 0.04 dB for active cladding alignment.

In this paper, we present a novel azimuthal alignment algorithm for multicore fiber splicing that separates the core and marker signals in side-view images. For two 4-core fiber designs, average splice losses of less than 0.03 dB are demonstrated using a 3-electrode arc-discharging fusion splicer, which are at the same level as single-core splice losses.

Side-view images, sinograms and algorithm

In the present study, we use the Fitel S185PM ROF fusion splicer hardware [11] and two different 4-core fiber designs with marker ("MCF1" and "MCF2"). For the example of MCF1, end-view and side-view images are shown in Fig. 1.

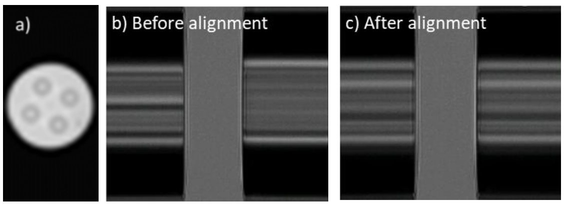

Fig. 1: MCF1. (a) End-view. (b) Side-view of both fiber ends before azimuthal alignment. (c) Side-view of both fiber ends after azimuthal alignment, showing a perfect match.

In the following, the angle ϑ denotes the azimuthal orientation of the fiber relative to the splicer camera plane in Fig. 1(b), z is the longitudinal location along the fiber, and x is the transverse coordinate parallel to the camera plane (x, z). Thus, Fig. 1(b) shows the side-view intensity $I(\vartheta, x, z)$ for one fixed orientation of the two fibers to be spliced. Choosing instead a fixed location, e.g., $z = z_\mathrm{L}$ close to the end of the left fiber, a *side-view sinogram* is the function $I(\vartheta, x, z_\mathrm{L})$ as shown in Fig. 2 , which is basically a series of one-dimensional cross-sectional intensity scans for many different azimuthal orientations of the fiber, e.g., each x-scan spaced 5° apart.

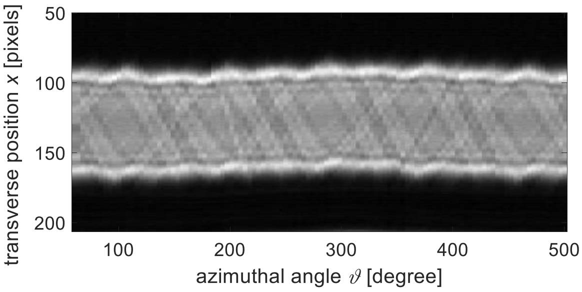

Fig. 2: Side-view sinogram $I(\vartheta, x, z_L)$ of MCF2, left fiber.

Correlating side-view sinograms that are taken near the ends $z = z_\mathrm{L}$ and $z = z_\mathrm{R}$ of the left and right fiber to be spliced, and integrating over the transverse coordinate x, we define the (global) cross-correlation

$$c(\vartheta) = \iint I(\vartheta', x, z_L) I(\vartheta' + \vartheta, x, z_R) \mathrm{d}\vartheta' \mathrm{d}x \quad (1)$$

The azimuthal spacing of the cores of both MCF1 (see Fig. 1) and MCF2 (see Fig. 2), as well as in the case of the MCF with four (outer) cores in [1] [4] [5] [6], is 90 degrees. Hence, there are $M_\mathrm{equiv} = 4$ equivalent ways (sectors, in this case quadrants) of aligning the cores before splicing. Consequently, the cross-correlation $c(\vartheta)$ from Eq.(1) has four distinct peaks in the example of MCF2 shown in Fig. 3(a). Since the marker is small compared to the cores, it has only a minor impact on the height of these peaks.

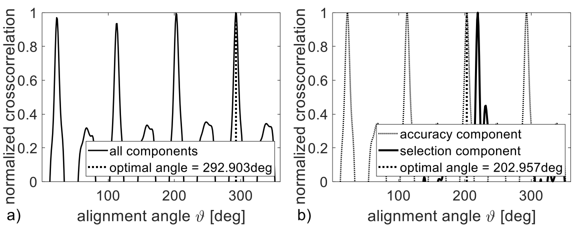

Fig. 3: Normalized cross-correlation of two fiber ends of MCF2. (a) Global, leading to wrong quadrant. (b) Separated into accuracy component and selection component, leading to correct quadrant.

To get a more robust signal from the marker, we separate the (Fast) Fourier Transform vector $\tilde{\boldsymbol{c}}$ of the cross-correlation $c(\vartheta)$ into an accuracy (cores) component $\tilde{\boldsymbol{c}}^{(\mathrm{acc})}$ and a selection (marker and other asymmetries) component $\tilde{\boldsymbol{c}}^{(\mathrm{sel})}$ according to

$$\tilde{\boldsymbol{c}} = \tilde{\boldsymbol{c}}^{(\mathrm{acc})} + \tilde{\boldsymbol{c}}^{(\mathrm{sel})}. \quad (2)$$

We choose the accuracy component vector $\tilde{\boldsymbol{c}}^{(\mathrm{acc})}$ such that it exclusively contains all harmonics (integer multiples) of the fundamental frequency M_equiv. Hence, its entries $\tilde{c}_n^{(\mathrm{acc})}$ are either zero or identical to the corresponding entries of the global cross-correlation according to

$$\tilde{c}_n^{(\mathrm{acc})} = \tilde{c}_n \quad \text{if} \quad n \in I^{(\mathrm{acc})}, \quad (3)$$

with $I^{(\mathrm{acc})}$ being the index set that contains all integer multiples of M_equiv, i.e.,

$$I^{(\mathrm{acc})} = n M_\mathrm{equiv}, \quad n \in \mathbb{Z}. \quad (4)$$

We note that the DC component is $\tilde{c}_0$ (as in C language, whereas it is $\tilde{c}_1$ in MATLAB®), and aliasing limits the range of the integer n in Eq. (4).

As expected, the inverse Fourier transform of $\tilde{\boldsymbol{c}}^{(\mathrm{acc})}$ (dotted in Fig. 3(b)) has the period $360°/M_\mathrm{equiv}$, i.e., it has in this case $M_\mathrm{equiv} = 4$ peaks of exactly identical height. The accurate azimuthal alignment angle is the location (in this case 202.957°) of that peak of the accuracy component that is closest to the single peak of the inverse Fourier transform of $\tilde{\boldsymbol{c}}^{(\mathrm{sel})}$ (solid in Fig. 3(b)). Instead, simply choosing the highest peak of the global cross-correlation $c(\vartheta)$ from Eq.(1) in Fig. 3(a) would have led us to the wrong quadrant (292.9°), i.e., a 90° error corresponding to a confusion of cores.

The fact that the peak of the selection component in Fig. 3(b) does not coincide with one of the peaks of the accuracy component in Fig. 3(b) shows that the markers of these two particular fibers cannot be simultaneously aligned with the cores. This means that these two fibers have the markers at different angles relative to the cores, either because of different fiber designs (marker locations) or a wrong relative polarity of the two fibers, i.e., one of the two fibers would need to be flipped to align the cores as well. In other words, the splitting method from Eq. (2) is robust against accidental or intentional flips of one or both fibers, as well as design differences. In contrast, the relative heights of the individual peaks of the global cross-correlation $c(\vartheta)$ from Eq.(1) in Fig. 3(a) are highly sensitive to such changes.

After the alignment computation, which is performed on a laptop that is connected to the splicer, one or both fibers are rotated by the total computed amount. An example after alignment is shown in Fig. 1(c). Finally, the two fibers are fusion-spliced using the three-electrode arc-discharging S185PM ROF splicer to achieve a uniform heat distribution across all cores, see Fig. 4.

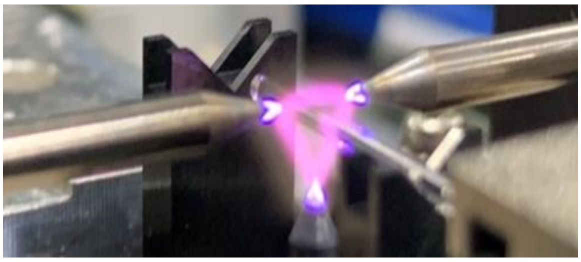

Fig. 4: 3-electrode splicing to achieve equal temperature and thus equally low loss for all cores.

Splice losses and speed

The side-view sinogram scan, alignment computation, rotation and arc time amount to only about 90 seconds with our new splicing solution. Splice losses for MCF1 and MCF2 are shown in Fig.5 for the fundamental mode at 1360nm wavelength. With an almost 100% alignment (correct core) success rate, we achieved average losses of 0.0185 dB (MCF1, correct polarity, 4 splices), 0.022 dB (MCF2, correct polarity, 10 splices) and 0.024 dB (MCF2, wrong polarity, 10 splices). Hence, regardless of polarity and for both fiber designs, the splice loss is at the same level as for single-core fiber splicing.

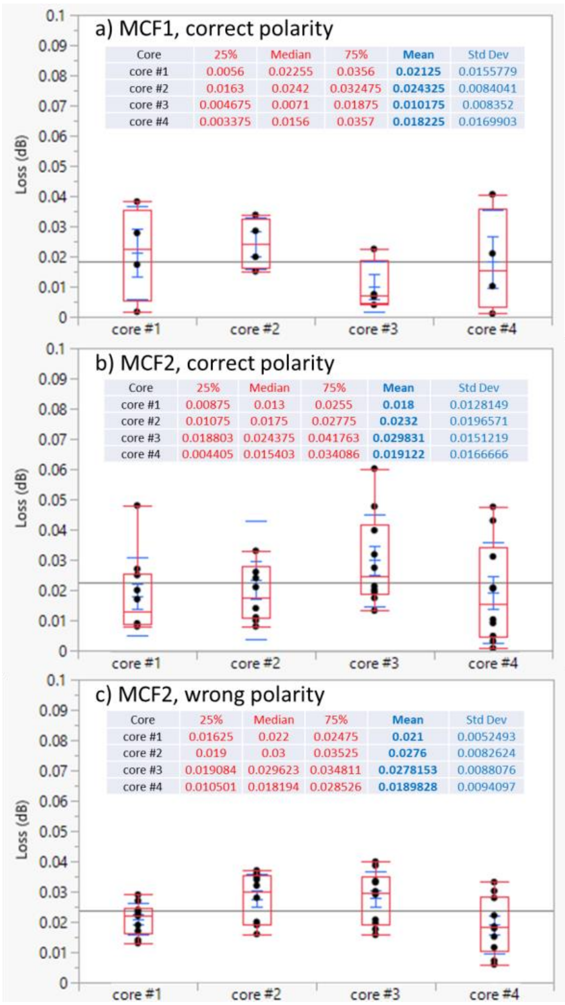

Fig. 5: Splice loss results when splicing identical fibers.

The standard deviations of the losses in Fig.5(a/b/c) are 0.012 dB, 0.016 dB and 0.0079dB, respectively, when averaging over the four cores (averages of the rightmost columns in the inserts in Fig.5). If we instead use the splice numbers as the horizontal axis in Fig.5, the standard deviations are only slightly smaller, with values of 0.010 dB, 0.012 dB and 0.0078 dB, respectively, when averaging over all performed splices in Fig.5(a/b/c). In other words, the splice loss is almost as uniform between splices as between cores, which confirms the high reliability of the proposed new azimuthal alignment method with the support of the 3-electrode arc-discharging splicer.

We note that these extremely low average loss values in Fig.5 are possible if there exists an azimuthal rotation for which all core locations of the two fibers to be spliced become identical, regardless how asymmetric the core locations are due to intentional or unintentional design features. If such a perfect alignment of all cores is geometrically impossible, e.g., because the two fibers have intentional or unintentional differences in their core locations, then the optimum alignment angle from our algorithm still gives the best possible average loss across all cores, but this loss will then be higher than in the identical-fiber case from Fig.5, depending on the amount of the differences of the core locations.

We further note that our alignment method can also be used for intentional offset clocking in long-haul MCF links to reduce channel differences in accumulated attenuation or to relax MCF manufacturing tolerances, by intentionally splicing together different cores. In this case, integer multiples of the azimuthal period $360°/M_{\mathrm{equiv}}$ are added to the computed optimum alignment angle, corresponding to selecting a different peak of the accuracy component.

Conclusion

A novel azimuthal alignment algorithm is presented for multicore and other fibers that are not circularly symmetric, e.g., polarization-maintaining fibers. The cross-correlation of the side-view sinograms of the two fibers to be spliced is separated into an accuracy component and a selection component. The selection component is used to select the correct peak of the accuracy component, which is then used to accurately quantify the optimum alignment angle. In combination with 3-electrode arc-discharging Fitel S185PM ROF splicer, we achieved an almost 100% alignment success rate with splicing times of only 90 seconds and single-core-fiber-like splice losses of less than 0.03 dB on average for two different 4-core fiber designs, regardless of polarity.

References

[1] K. Saito, T. Sakamoto, T. Matsui, K. Nakajima and T. Kurashima, "Side-view based angle alignment technique for multi-core fiber," *Optical Fiber Communications Conference (OFC),* paper M3F.3, 2016, DOI: https://doi.org/10.1364/OFC.2016.M3F.3

[2] W. Zheng, "Automated alignment and splicing for multicore fibers," *Optical Fiber Communications Conference (OFC),* paper OM3I.4, 2013, DOI: https://doi.org/10.1364/OFC.2013.OM3I.4

[3] W. Zheng, D. Duke, T. Kubo, and B. Malinsky, "Interrelation profile analysis method for alignment of polarization-maintaining fiber," *Optical Fiber Communications Conference (OFC),* paper JThA61, 2010, DOI: https://doi.org/10.1364/NFOEC.2010.JThA61

[4] M. Ohzeki, "Alignment and fusion splicing techniques for MCFs," *European Conference on Optical Communication (ECOC)*, Workshop Mo1A-WS, 2021

[5] M. Ohzeki, Y. Sasaki, K. Takenaga, K. Ichii and K. Aikawa, "Side-view rotational alignment method for trench-assisted 4-core fibers," *Optical Fiber Communications Conference (OFC),* paper M4E.4, 2022, DOI: https://doi.org/10.1364/OFC.2022.M4E.4

[6] M. Takahashi, T. Fujii, R. Sugizaki, M. Tsukamoto and Y. Arashitani, "Field usable fusion splicing technique for multicore fiber," *IEEE Photonics Society Summer Topicals Meeting (SUM), 2020*, DOI: https://doi.org/10.1109/SUM48678.2020.9161043

[7] W. Ji, R. Yu, Z. Shen, C. Wang, C. Xiong and L. Xiao, “Low-loss fusion splicing between spacing-mismatched multicore fibers”, *Optics. Letters*, vol. 46, no. 24, pp. 6112–6115, 2021, DOI: https://doi.org/10.1364/OL.447602

[8] M. Suzuki, H. Yoshii, T. Ito, Y. Yamamoto, T. Hayashi and T. Hasegawa, "Low loss splicing between coupled multi-core fibers with thermally expanded cores," *Optical Fiber Communications Conference (OFC),* paper Tu3B.5, 2018, DOI: https://doi.org/10.1364/OFC.2018.Tu3B.5

[9] W. Zheng, H. Sugawara and B. Malinsky, "Fourier analysis method for asymmetric polarization-maintaining fiber," *Optical Fiber Communications Conference (OFC),* paper JW2A.12, 2012, DOI: https://doi.org/10.1364/NFOEC.2012.JW2A.12

[10] Y. Amma, A. Takahashi, K. Takenaga and S. Matsuo, "Accuracy of core alignment with end-view function for multicore fiber," *IEEE Photonics Society Summer Topicals Meeting (SUM), 2014*, DOI: https://doi.org/10.1109/SUM.2014.94

[11] https://www.furukawa.co.jp/splicer/en/product/s185pmrof.html